



Supplement of

An evaluation of the heat test for the ice-nucleating ability of minerals and biological material

Martin I. Daily et al.

Correspondence to: Martin I. Daily (m.i.daily1@leeds.ac.uk) and Benjamin J. Murray (b.j.murray@leeds.ac.uk)

The copyright of individual parts of the supplement might differ from the article licence.

Supplementary Information

S1 Background information on classes of mineral INPs

S1.1 K-feldspar

Alkali feldspars rich in potassium (K-feldspars) are considered to be the most important single ice-nucleating mineral component in atmospheric mineral dust due to their exceptional ability to nucleate ice in both immersion (Atkinson et al., 2013; Zolles et al., 2015; Harrison et al., 2019) and deposition mode (Yakobi-Hancock et al., 2013) in combination with its ubiquitous atmospheric abundance (Arnold et al., 1998; Murray et al., 2012; Glaccum and Prospero, 1980; Kandler et al., 2009). As such, even in the presence of other minerals in higher proportions, the INA of a mineral dust will likely be controlled by the K-feldspar content (Harrison et al., 2016). Ice nucleation on mineral surfaces such as feldspars has been shown to occur at specific sites that become active at a specific temperature (Holden et al., 2019; Holden et al., 2021) and topographical features associated with exsolution microtexture (Whale et al., 2017; Kiselev et al., 2021) have been proposed as the locations of the highly active sites on K-feldspar. Moreover, Kiselev et al. (2017) observed that ice crystals growing from the vapour phase on the surface of microcline originated on steps and cracks and were preferentially orientated between the basal face of ice and the (100) cleavage plane. More recent work suggests that cracks caused by exsolution microtexture may expose the (100) face of feldspars (Kiselev et al., 2021). The chemical and physical nature of these sites is, however, still unclear.

S1.2 Plagioclase feldspar

Plagioclase feldspars are the most abundant mineral in the Earth's crust and are defined as having feldspar compositions between that of the Na endmember albite ($\text{NaAlSi}_3\text{O}_8$) and the Ca endmember anorthite ($\text{CaAl}_2\text{Si}_2\text{O}_8$). Solid solutions between these two endmembers are more stable than in alkali feldspars, therefore plagioclase feldspars do not exhibit the 'perthitic' texture (exsolution microtexture) characteristic of K-feldspars. It has been suggested that the lack of these textures is the reason (Whale et al., 2017) that plagioclase feldspars are typically much less efficient INPs than K-feldspars (Harrison et al., 2016).

S1.3 Silica

Quartz is the most common crustal mineral after the feldspars and is also highly chemically and physically resistant to weathering. It is often a major component of soils and sediments and is the most abundant non-phyllosilicate mineral component of atmospheric mineral dust (Arnold et al., 1998; Murray et al., 2012; Glaccum and Prospero, 1980; Kandler et al., 2009). Quartz is the crystalline form of silica (SiO_2) and occurs in nature as several different polymorphs. However, α -quartz is by far the most abundant polymorph and as such is usually referred to as 'quartz'. Previous laboratory studies have indicated that quartz particles have an atmospheric importance as INPs superior to that of clays but lower than alkali and plagioclase feldspars (Atkinson et al., 2013; Harrison et al., 2019), although there is variability in INA seen between different studies (Kumar et al., 2019a).

Re-milling quartz powders has been seen to enhance their INA more than what may be expected based on the increase in surface area (Zolles et al., 2015), suggesting that the process creates active sites rather than simply exposing them. This has led to uncertainty as to whether the documented INA of quartz is representative of that found in the environment or whether it is simply an artefact of the laboratory milling process. The active sites of quartz are proposed to arise from fracturing that produce patches of ‘dangling’ Si- and Si-O sites on the mineral surface that can readily hydroxylate and order water molecules. Another characteristic of quartz is that it can lose its INA while immersed in room temperature water over a few days (Kumar et al., 2019a; Harrison et al., 2019).

S1.4 Clay-based minerals

Clay minerals are present in abundance in soils, sedimentary and some metamorphic rocks, as well as in airborne samples of mineral dust. Clays fall into the phyllosilicate group of minerals, with its principal subgroups comprising kaolin (which includes kaolinite), smectite (which includes montmorillonite), illite and chlorite. They are secondary minerals, meaning that they are weathering products of igneous and metamorphic minerals and, as such, samples often contain relic traces of their parent minerals (for example K-feldspar in the case of kaolinite or illite) and also of quartz as a weathering reaction product. Clays were previously considered (Hoose and Möhler, 2012) to be the most important mineral ice-nucleating component of atmospheric mineral dust owing to early experimental work (Mason and Maybank, 1958) until the greater importance of feldspars was established (Atkinson et al., 2013). They are, however, still overall the most abundant type of mineral found in atmospheric mineral dust, their concentration tending to increase proportionally in transported dusts owing to their smaller particle size (Murray et al., 2012). Therefore, clay minerals may be more likely to control the INA of desert dusts sampled far from their source and of the finer particle fraction.

S1.5 Mineral dust analogues

Mineral dust analogue samples NX Illite and Arizona Test Dust (ATD) are two commercially available mineral dust mixtures that have been used as atmospheric mineral dust analogues in laboratory investigations into the properties of INPs (Marcolli et al., 2007; Broadley et al., 2012; Niemand et al., 2012; Hiranuma et al., 2015a). ATD contains a much higher proportion (~50 %) of quartz and feldspars than NX Illite (~20 %), with the remainder of both comprising clay minerals and a small amount of carbonate. It has been suggested that the INA of ATD may be artificially enhanced by the milling process used in its production (Perkins et al., 2020). Both mineral dust samples contain a higher proportion of K-feldspar than quartz (Broadley et al., 2012; Hiranuma et al., 2015a) meaning that K-feldspar should be the main contributor to the INA of both samples. This is consistent with the relatively high INA of ATD, in which the dominant polymorph of K-feldspar is microcline (Kaufmann et al., 2016). However, NX Illite is less active than would be expected given its K-feldspar content, which may be due to weathering or that the K-feldspar may have an INA at the lower end of the K-feldspar INA range (Harrison et al., 2016).

S1.6 Calcite

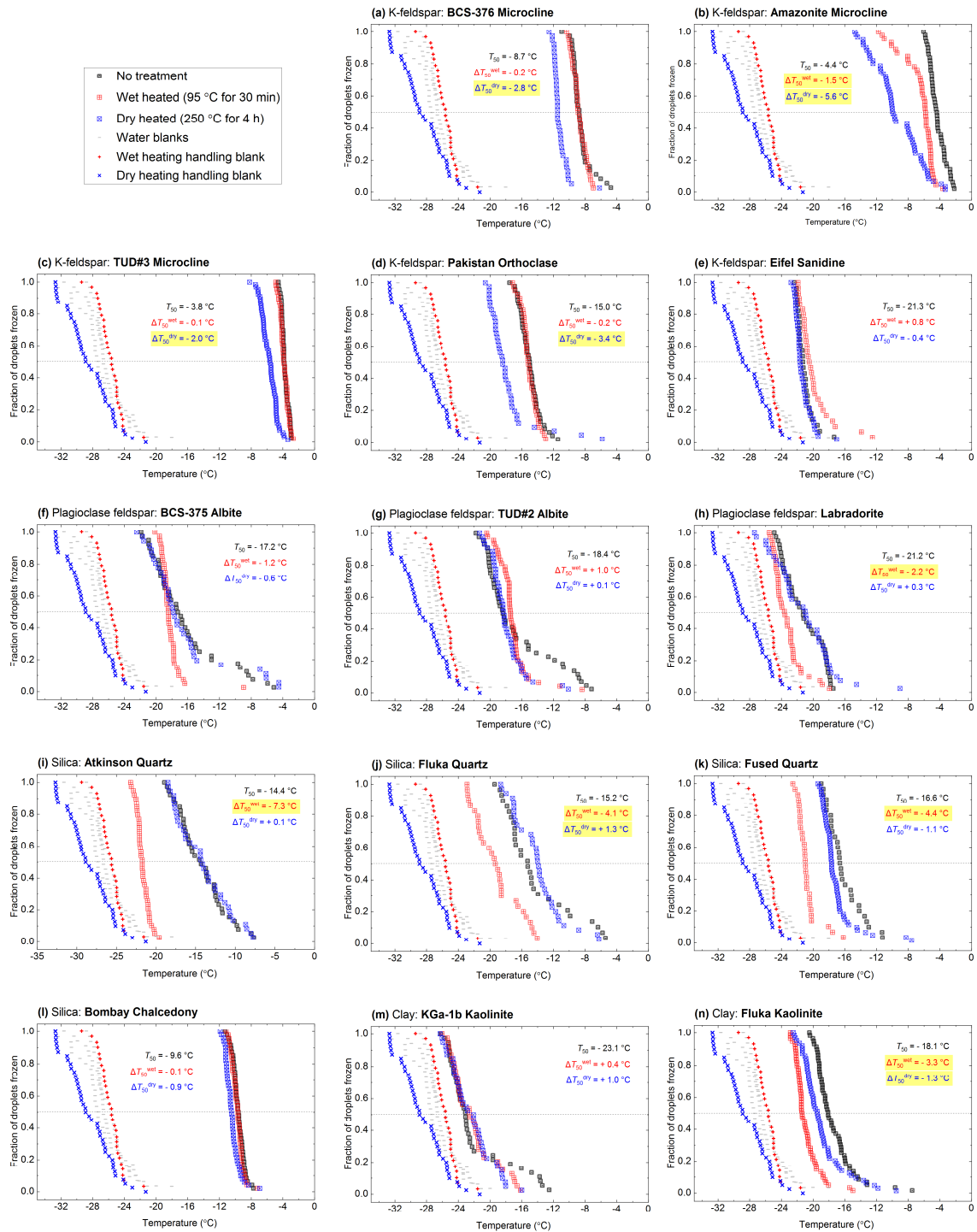
Calcite (CaCO_3), along with other carbonates such as gypsum and dolomite, has been found to be an ineffective mineral INP (Atkinson et al., 2013; Zolles et al., 2015; Kaufmann et al., 2016), however it can often be the dominant component of some surface dust sources, especially the deserts of north-western Africa (Knippertz and Stuut, 2014).

S2 Mass changes of samples after dry heating

Table S1: Mass changes of samples after dry heat treatment (250 °C for 4 h)

Sample name	Classification	% Change in mass after dry heating (250 °C for 4 h)
Empty 15 mL borosilicate glass vial (mean of 5)	-	-0.02 (mean) 0.10 (standard deviation)
BCS-376 Microcline (mean of 5)	K-feldspar	-0.25 (mean) 0.44 (standard deviation)
TUD#3 Microcline	K-feldspar	-2.53
Amazonite Microcline	K-feldspar	-0.68
Pakistan Orthoclase	K-feldspar	-0.96
TUD#2 Albite	Plagioclase feldspar	-1.39
BCS-375 Albite	Plagioclase feldspar	-2.32
Atkinson Quartz	Quartz	
Fluka Quartz (mean of 5)	Quartz	-0.27 (mean) 0.52
Fused Quartz	Quartz	-1.72
Bombay Chalcedony	Quartz	-0.59
KGa-1b Kaolinite	Clay-based	-1.01
Fluka Kaolinite	Clay-based	-0.78
Sigma Montmorillonite	Clay-based	-10.01
SWy-2 Montmorillonite	Clay-based	-8.44
Chlorite	Clay-based	
Arizona Test Dust (ATD)	Dust surrogate	-1.57
NX Illite	Dust surrogate	-3.47
Calcite	Carbonate	-3.40
Snomax (pellets)	Biological heat-sensitive	-37.4
Lichen (raw)	Biological heat-sensitive	-58.8
Birch Pollen (raw)	Biological heat-resistant	-56.3
Microcrystalline cellulose	Biological heat-resistant	-52.6

S3 Supplementary figures



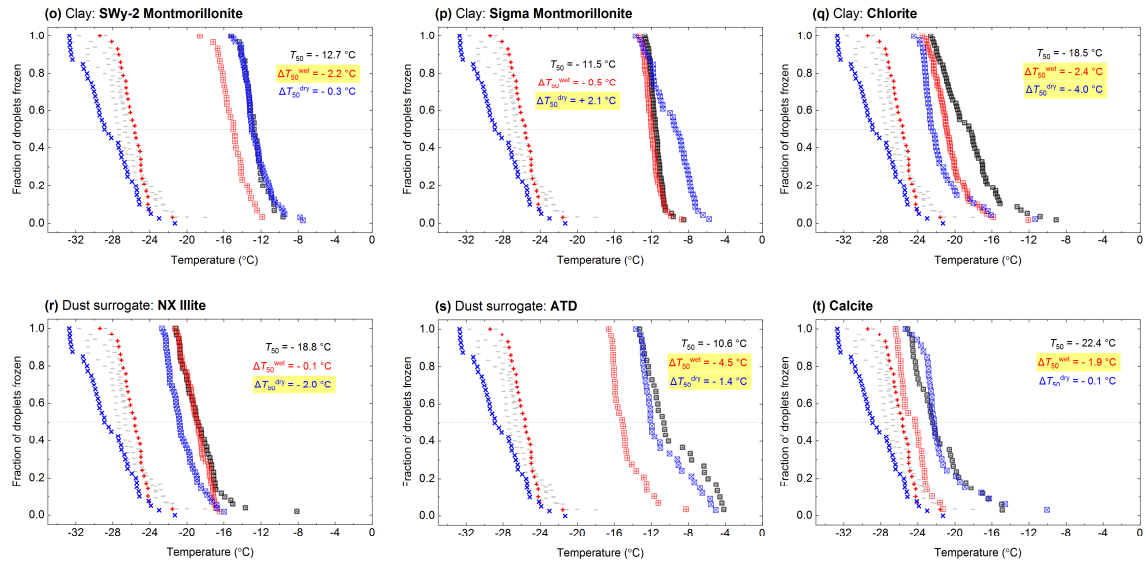


Figure S1: Fraction of droplets frozen ($f_{\text{ice}}(T)$) curves for all mineral-based INP samples. Data for three clean water blanks runs along with wet and dry heating handling blanks are shown in each plot. A dotted horizontal line denotes $f_{\text{ice}}(T) = 0.5$, from which T_{50} values were determined. All suspensions were prepared to a concentration of 1 % w/v. Denoted in each panel are T_{50} , $\Delta T_{50}^{\text{wet}}$ and $\Delta T_{50}^{\text{dry}}$ values for the sample, with significant (ΔT_{50} greater than $\pm 1.2\text{ }^{\circ}\text{C}$) values highlighted in yellow.

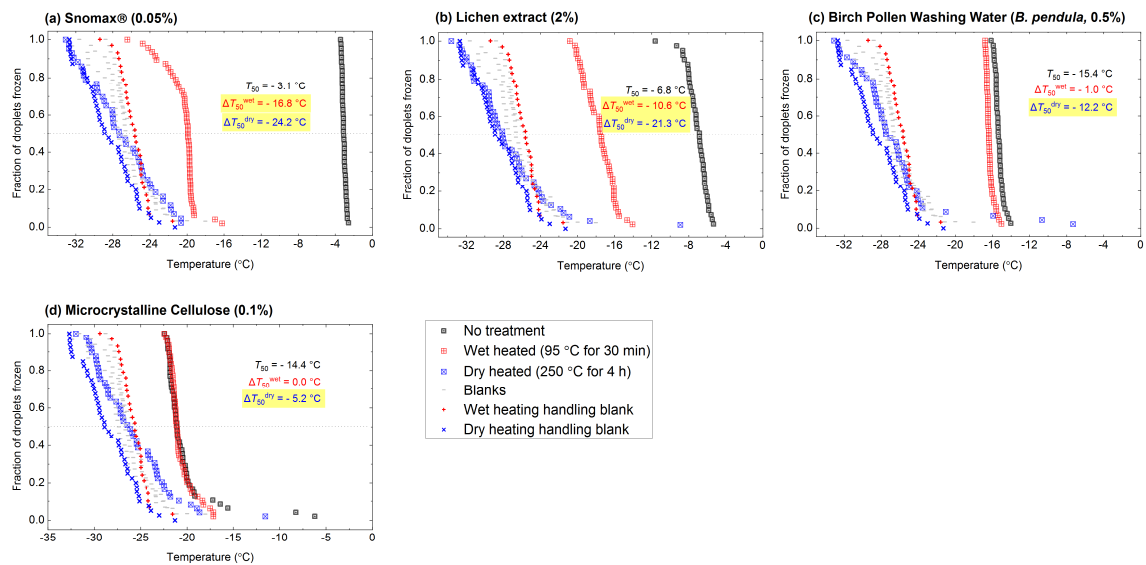


Figure S2: Fraction of droplets frozen ($f_{\text{ice}}(T)$) curves for all biological INP samples. Data for three clean water blanks runs along with wet and dry heating handling blanks are shown in each plot. A dotted horizontal line denotes $f_{\text{ice}}(T) = 0.5$, from which T_{50} values were determined. All suspensions were prepared to a concentration of 1 % w/v. Denoted in each panel are T_{50} , $\Delta T_{50}^{\text{wet}}$ and $\Delta T_{50}^{\text{dry}}$ values for the sample, with significant (ΔT_{50} greater than $\pm 1.2\text{ }^{\circ}\text{C}$) values highlighted in yellow.

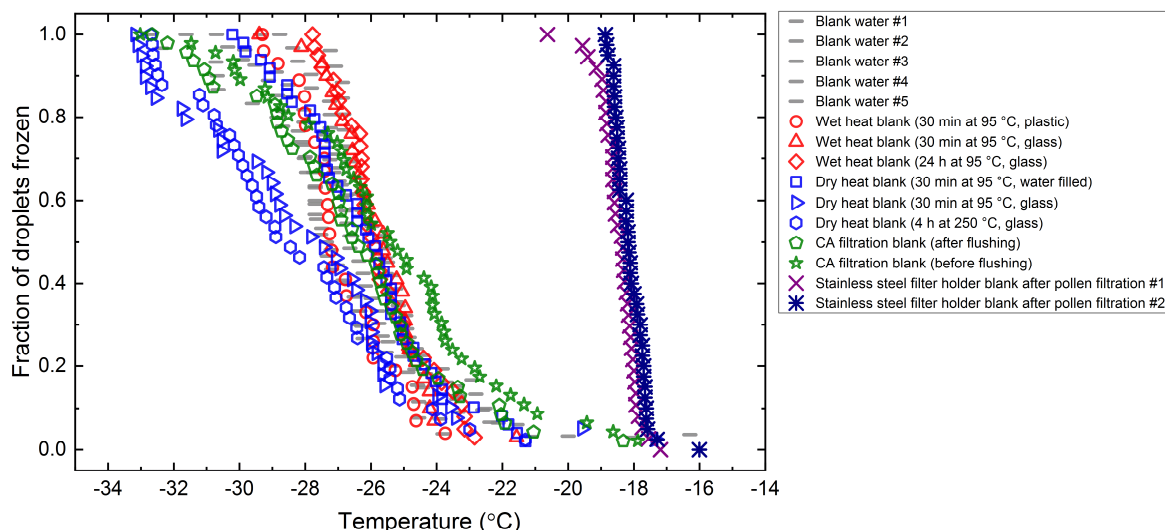


Figure S3: Plot showing $f_{ice}(T)$ data for background water in borosilicate glass vials (Blanks #1 to #5) and handling blanks for various modes of wet and dry heat tests in borosilicate and polypropylene containers. ‘CA’ denotes the use of a 0.2 μm cellulose acetate filter used for filtration of raw lichen and birch pollen.

References to Supplement

Arnold, E., Merrill, J., Leinen, M., and King, J.: The effect of source area and atmospheric transport on mineral aerosol collected over the North Pacific Ocean, *Global. Planet. Change.*, 18, 137-159, [https://doi.org/10.1016/S0921-8181\(98\)00013-7](https://doi.org/10.1016/S0921-8181(98)00013-7), 1998.

Atkinson, J. D., Murray, B. J., Woodhouse, M. T., Whale, T. F., Baustian, K. J., Carslaw, K. S., Dobbie, S., O’Sullivan, D., and Malkin, T. L.: The importance of feldspar for ice nucleation by mineral dust in mixed-phase clouds, *Nature*, 498, 355-358, [10.1038/nature12278](https://doi.org/10.1038/nature12278), 2013.

Augustin-Bauditz, S., Wex, H., Kanter, S., Ebert, M., Niedermeier, D., Stolz, F., Prager, A., and Stratmann, F.: The immersion mode ice nucleation behavior of mineral dusts: A comparison of different pure and surface modified dusts, *Geophys. Res. Lett.*, 41, 7375-7382, <https://doi.org/10.1002/2014GL061317>, 2014.

Glaccum, R. A., and Prospero, J. M.: Saharan aerosols over the tropical North Atlantic — Mineralogy, *Mar. Geol.*, 37, 295-321, [https://doi.org/10.1016/0025-3227\(80\)90107-3](https://doi.org/10.1016/0025-3227(80)90107-3), 1980.

Harrison, A. D., Whale, T. F., Carpenter, M. A., Holden, M. A., Neve, L., amp, apos, Sullivan, D., Vergara Temprado, J., and Murray, B. J.: Not all feldspars are equal: a survey of ice nucleating properties across the feldspar group of minerals, *Atmos. Chem. Phys.*, 16, 10927-10940, [10.5194/acp-16-10927-2016](https://doi.org/10.5194/acp-16-10927-2016), 2016.

Harrison, A. D., Lever, K., Sanchez-Marroquin, A., Holden, M. A., Whale, T. F., Tarn, M. D., McQuaid, J. B., and Murray, B. J.: The ice-nucleating ability of quartz immersed in water and its atmospheric importance compared to K-feldspar, *Atmos. Chem. Phys.*, 19, 11343-11361, [10.5194/acp-19-11343-2019](https://doi.org/10.5194/acp-19-11343-2019), 2019.

Hiranuma, N., Augustin-Bauditz, S., Bingemer, H., Budke, C., Curtius, J., Danielczok, A., Diehl, K., Dreischmeier, K., Ebert, M., Frank, F., Hoffmann, N., Kandler, K., Kiselev, A., Koop, T., Leisner, T., Möhler, O., Nillius, B., Peckhaus, A., Rose, D., Weinbruch, S., Wex, H., Boose, Y., DeMott, P. J., Hader, J. D., Hill, T. C. J., Kanji, Z. A., Kulkarni, G., Levin, E. J. T., McCluskey, C. S., Murakami, M., Murray, B. J., Niedermeier, D., Petters, M. D., O'Sullivan, D., Saito, A., Schill, G. P., Tajiri, T., Tolbert, M. A., Welti, A., Whale, T. F., Wright, T. P., and Yamashita, K.: A comprehensive laboratory study on the immersion freezing behavior of illite NX particles: a comparison of 17 ice nucleation measurement techniques, *Atmos. Chem. Phys.*, 15, 2489-2518, 10.5194/acp-15-2489-2015, 2015a.

Holden, M. A., Whale, T. F., Tarn, M. D., O'Sullivan, D., Walshaw, R. D., Murray, B. J., Meldrum, F. C., and Christenson, H. K.: High-speed imaging of ice nucleation in water proves the existence of active sites, *Sci Adv*, 5, eaav4316, 10.1126/sciadv.aav4316, 2019.

Holden, M. A., Campbell, J. M., Meldrum, F. C., Murray, B. J., and Christenson, H. K.: Active sites for ice nucleation differ depending on nucleation mode, *P. Nat. Acad. Sci. USA.*, 118, e2022859118, 10.1073/pnas.2022859118, 2021.

Hoose, C., and Möhler, O.: Heterogeneous ice nucleation on atmospheric aerosols: a review of results from laboratory experiments, *Atmos. Chem. Phys.*, 12, 9817-9854, 10.5194/acp-12-9817-2012, 2012.

Kandler, K., SchütZ, L., Deutscher, C., Ebert, M., Hofmann, H., JäCkel, S., Jaenicke, R., Knippertz, P., Lieke, K., Massling, A., Petzold, A., Schladitz, A., Weinzierl, B., Wiedensohler, A., Zorn, S., and Weinbruch, S.: Size distribution, mass concentration, chemical and mineralogical composition and derived optical parameters of the boundary layer aerosol at Tinfou, Morocco, during SAMUM 2006, *Tellus B: Chemical and Physical Meteorology*, 61, 32-50, 10.1111/j.1600-0889.2008.00385.x, 2009.

Kaufmann, L., Marcolli, C., Hofer, J., Pinti, V., Hoyle, C. R., and Peter, T.: Ice nucleation efficiency of natural dust samples in the immersion mode, *Atmos. Chem. Phys.*, 16, 11177-11206, 10.5194/acp-16-11177-2016, 2016.

Kiselev, A., Keinert, A., Gaedecke, T., Leisner, T., Sutter, C., Petrishcheva, E., and Abart, R.: Effect of chemically induced fracturing on the ice nucleation activity of alkali feldspar, *Atmos. Chem. Phys. Discuss.*, 2021, 1-17, 10.5194/acp-2021-18, 2021.

Knippertz, P., and Stuut, J.: Mineral Dust: A Key Player in the Earth System, *Mineral Dust*, 2014.

Kumar, A., Marcolli, C., and Peter, T.: Ice nucleation activity of silicates and aluminosilicates in pure water and aqueous solutions – Part 2: Quartz and amorphous silica, *Atmos. Chem. Phys.*, 19, 6035-6058, 10.5194/acp-19-6035-2019, 2019a.

Murray, B. J., O'Sullivan, D., Atkinson, J. D., and Webb, M. E.: Ice nucleation by particles immersed in supercooled cloud droplets, *Chem Soc Rev*, 41, 6519-6554, 10.1039/c2cs35200a, 2012.

Yakobi-Hancock, J. D., Ladino, L. A., and Abbatt, J. P. D.: Feldspar minerals as efficient deposition ice nuclei, *Atmos. Chem. Phys.*, 13, 11175-11185, 10.5194/acp-13-11175-2013, 2013.

Whale, T. F., Holden, M. A., Kulak, A. N., Kim, Y. Y., Meldrum, F. C., Christenson, H. K., and Murray, B. J.: The role of phase separation and related topography in the exceptional ice-nucleating ability of alkali feldspars, *Phys Chem Chem Phys*, 19, 31186-31193, 10.1039/c7cp04898j, 2017.

Zolles, T., Burkart, J., Hausler, T., Pummer, B., Hitzenberger, R., and Grothe, H.: Identification of ice nucleation active sites on feldspar dust particles, *J Phys Chem A*, 119, 2692-2700, 10.1021/jp509839x, 2015.